Published in final edited form as:
Reproduction. 2014 May ; 147(5): 615–625. doi:10.1530/REP-13-0304.

The small GTPase Rheb is required for spermatogenesis but not oogenesis

MD Baker[1,2], **M Ezzati**[3], **GM Aloisio**[1], **ED Tarnawa**[3], **I Cuevas**[1], **Y Nakada**[1], and **DH Castrillon**[1,4]

[1]Department of Pathology, University of Texas Southwestern Medical Center, Dallas, TX

[3]Department of Obstetrics & Gynecology, Division of Reproductive Endocrinology & Infertility, University of Texas Southwestern Medical Center, Dallas, TX

Abstract

The process of germ cell development is under the tight control of various signaling pathways among which the PI3K-Akt-mTOR pathway is of critical importance. Previous studies have demonstrated sex-specific roles for several components of this pathway. In the current study we aimed to evaluate the role of Rheb, a member of the small GTPase superfamily and a critical component for mTORC1 activation, in male and female gametogenesis. The function of Rheb in development and the nervous system has been extensively studied, but little is known about its role in the germline. We have exploited genetic approaches in the mouse to study the role of Rheb in the germline and have identified an essential role in spermatogenesis. Conditional knockout (cKO) of *Rheb* in the male germline resulted in severe oligoasthenoteratozoospermia and male sterility. More detailed phenotypic analyses uncovered an age-dependent meiotic progression defect combined with subsequent abnormalities in spermiogenesis as evidenced by abnormal sperm morphology. In the female, however, germ-cell specific inactivation of *Rheb* was not associated with any discernible abnormality; these cKO mice were fertile with morphologically unremarkable ovaries, normal primordial follicle formation, and subsequent follicle maturation. The absence of an abnormal ovarian phenotype is striking given previous studies demonstrating a critical role for the mTORC1 pathway in the maintenance of primordial follicle pool. In conclusion, our findings demonstrate an essential role of *Rheb* in diverse aspects of spermatogenesis but suggest the existence of functionally-redundant factors that can compensate for *Rheb* deficiency within oocytes.

Introduction

The PI3K/AKT/mTOR signaling pathway is highly conserved among diverse species and plays important roles in the regulation of cell growth. Among other functions, this pathway serves as a key mediator for cellular responses to both the environment and the intracellular

[4]Correspondence: Diego H. Castrillon, Department of Pathology, University of Texas Southwestern Medical Center, 6000 Harry Hines Blvd., Dallas, TX 75390-9072. Phone: 214.648.4032; Fax: 214.648.7355; Diego.Castrillon@UTSouthwestern.edu.
[2]Current address – Fort Worth Fertility 1800 Mistletoe Blvd, Fort Worth, TX 76104

Declaration of Interests
The authors have no conflicts of interest to declare.

milieu, including growth factors, nutrient availability, oxygen levels and intracellular energy charge (Laplante & Sabatini 2009). Working through this pathway, these environmental and intracellular signals exert many changes in cellular physiology to maintain homeostasis. Among these, changes in the rate of protein translation and turnover, and cell cycle progression, are among the best characterized(Laplante & Sabatini 2009).

The cell survival and growth kinase PI3K represents one important node of this pathway. PI3K converts membrane bound phosphatidylinositol 4,5-bisphosphate (PIP2) to phosphatidylinositol (3,4,5)-trisphosphate (PIP3). PIP3 acts as a second messenger by membrane-recruitment and activation of the serine-threonine kinase Akt. Pten, a powerful inhibitor of PI3K signaling, acts to convert PIP3 back to PIP2, thereby suppressing Akt activation. Akt in turn phosphorylates and thereby inhibits Tsc2, and also phosphorylates many additional downstream targets including the Foxo transcription factors, which also play multiple roles in cell growth and proliferation (John *et al.* 2008, Goertz *et al.* 2011, Tzivion *et al.* 2011). The AMP kinase AMPK is another important node of this pathway acting via Tsc2. AMPK is activated by energy stress/low nutrient levels (which result in high intracellular levels of AMP) and also phosphorylates Tsc2. Tsc2 can also be phosphorylated by additional kinases (e.g. Redd1, Erk, Ikkβ) in response to other environmental cues (Laplante & Sabatini 2009). Tsc2 and its physical partner, Tsc1 are structurally unrelated, but form an obligate complex whose principal (and indeed, only well-documented) role is as negative regulator (via Rheb) of mTORC1 (one of the two physically and functionally distinct signaling complexes in which mTOR is a key component, the other being mTORC2). The only known function of Tsc1 is to stabilize Tsc2 and prevent its degradation.

Rheb is a small GTPase and member of the Ras family and is ubiquitously expressed in mammals. Tsc2 contains a GAP (GTPase-activating) domain that stimulates the intrinsic GTPase activity of Rheb, thereby promoting the conversion of Rheb-GTP into Rheb-GDP. Whereas Rheb-GTP potently activates mTORC1, Rheb-GDP is inactive. Rheb directly activates mTORC1 through mechanisms that are not well-understood. These findings are based on numerous genetic and biochemical studies performed in vertebrate and vertebrate model systems and appear to be universal. For example, in *Tsc1* or *Tsc2* mutant cells, mTORC1 is constitutively active, potently stimulating cell growth (Fingar & Blenis 2004, Zou *et al.* 2011).

mTORC1 in turn regulates protein translation largely through two proteins that are key components of the translational control machinery, ribosomal protein S6 (S6) and 4E Binding Protein (4EBP), to potently drive protein translation and cell growth. Phosphorylation of p70S6 kinase (S6K) results in the activation of S6, which allows for the formation of the mRNA translation machinery. mTORC1 also increases protein synthesis by inactivating the translational repressor 4EBP which binds to and inhibits the eukaryotic translation initiation factor 4E (eIF4E) (Laplante & Sabatini 2009).

Several studies have implicated some of these key components of the PI3K/AKT/mTOR pathway in spermatogenesis and oogenesis. Foxo1 is specifically expressed in undifferentiated spermatogonia, and the three Foxos together regulate multiple steps of

spermatogenesis including stem cell maintenance and differentiation (Goertz *et al.* 2011, Tarnawa *et al.* 2013). *Pten* is also required for spermatogenesis; its inactivation with the germline-specific *Vasa-Cre* (Gallardo *et al.* 2007a) results in severe defects in spermatogonial maintenance and differentiation, at least in part through Foxo1 (Goertz *et al.* 2011). Other studies have implicated mTORC1 as a regulator of spermatogenesis and spermatogonial stem cell maintenance (Hobbs *et al.* 2010).

In the ovary, *Foxo3* is specifically expressed in primordial oocytes, where it serves to potently restrain their activation. In *Foxo3*-null mice, primordial follicles develop normally, but undergo global activation immediately after they are formed, resulting in a syndrome of deregulated follicle growth and premature female infertility (Castrillon *et al.* 2003, Hosaka *et al.* 2004, John *et al.* 2007, John *et al.* 2008). Strikingly, an identical ovarian phenotype occurs following conditional germline inactivation of three other PI3K/AKT/mTOR pathway components: *Pten*, *Tsc1*, and *Tsc2*, underscoring the importance of this pathway in the maintenance of the female germline (John *et al.* 2008, Reddy *et al.* 2008, Adhikari *et al.* 2009, Adhikari *et al.* 2010). *Pten* inactivation results in global primordial follicle activation through Akt and consequent phosphorylation and cytoplasmic sequestration/inactivation of Foxo3 (John *et al.* 2008). *Tsc1* and *Tsc2* inactivation in oocytes results in global primordial activation associated with mTOR pathway hyperactivity and increased phosphorylation of S6K and 4EBP within oocytes (Adhikari *et al.* 2009, Adhikari *et al.* 2010). These recent mouse models have laid the groundwork for uncovering the regulation of primordial follicle maintenance but further investigations are required to identify how these canonical PI3K branch components (Pten, Akt, Foxos) interact with canonical mTOR branch components (Tsc1/Tsc2) (Sullivan & Castrillon 2011). To further explore these questions and the role of mTOR signaling in gametogenesis, we studied the impact of *Rheb* inactivation in both the male and female germline.

Materials and Methods

Mouse strains, breeding, and tissue processing and expression analyses

This study was approved by the University of Texas Southwestern Medical Center Institutional Animal Care and Use Committee. Generation of both the *Rheb* floxed and *Vasa-Cre* alleles and genotyping protocols were previously described (Gallardo *et al.* 2007a, Zou *et al.* 2011). *Vasa-Cre* males were crossed with $Rheb^{f/f}$ females. *Vasa-Cre;* $Rheb^{f/+}$ male offspring were again crossed to $Rheb^{f/f}$ females to produce *Vasa-Cre;* $Rheb^{f/-}$ experimental mice. Matched *Vasa-Cre* negative siblings were used as controls. All tissues were processed immediately after procurement. Tissues were fixed in 10% neutral buffered formalin for 24 hours, embedded in paraffin, and cut into 5-μm sections for IHC or H&E staining. Tissue sections from experimental and control samples were placed on the same slide to ensure identical processing. Expression analyses by digital Northern were conducted as previously described (Gallardo *et al.* 2007b).

Sperm analysis and breeding assays

A complete sperm analysis was performed to quantify the output of the testis. Epididymal sperm density was obtained by counting the number of hematoxylin stained sperm heads in

three 20x fields for each epididymis. The area in the seminiferous tubule was calculated using the ImageJ software package (Schneider *et al.* 2012). Data was graphed as total sperm per square pixel. Epididymal sperm concentration was used as a secondary measure of total sperm output. One epididymis was dissected and placed into one ml of phosphate buffered solution. Approximately 5 cuts were made in the epididymis followed by thirty minute incubation at 37°C to release the sperm from the tissue. Sperm concentration was then measured using a fixed cover slip counting chamber (Cell-Vu, DRM-600). Motility was also noted but experimental samples contained too few sperm for percentages to be accurately calculated. To study sperm morphology, a small drop of the sperm suspension was placed on a glass microscope slide and was spread evenly across the slide with a cover slip. The sperm smear was allowed to dry and was then subjected to Diff-Quik staining (Harleco, 65044C). Previously published criteria were used for the determination of normal sperm morphology (Wyrobek & Bruce 1975). Breeding assays were performed as previously described (Gallardo *et al.* 2008). Three week-old experimental and sibling control males were placed with two six week-old FVB females and observed for 20 weeks. Females were placed with one FVB male and observed for 18 weeks.

Immunohistochemistry and quantitative analyses of morphology in tissue sections

Slides were deparaffinized in xylene, hydrated in an ethanol series, subjected to antigen retrieval by boiling in 10 mM sodium citrate (pH 6.0) for 15 min, and cooled at room temperature (RT) for 20 min. After peroxidase blocking (3% hydrogen peroxide in water) for 30 min, slides were washed in water and then blocked in bovine serum albumin (BSA, 1% in 1x PBS) for 15 min. Slides were then incubated with primary antibody overnight at 4°C, subjected to a TBST (1 M Tris-HCL, 5 M NaCl, 1x Tween-20) wash series, incubated with secondary antibody for 30 min at RT (Immpress; Vector Laboratories), and subjected to a second TBST wash series. Signal was detected using a DAB liquid chromogen substrate kit (DAKO). Slides were then counterstained with hematoxylin, rinsed in water, and air-dried. Antibodies and titers used included Foxo1 (rabbit monoclonal; Cell Signaling Technology, #2880; 1:500), Crem1 (rabbit polyclonal; Santa Cruz Biotechnology, #SC-440; 1:1000), mTOR (rabbit monoclonal; Cell Signaling Technology, #2983; 1:1000), p-mTOR (rabbit monoclonal; Cell Signaling Technology, #5536; 1:1000), p-4EBP (rabbit monoclonal; Cell Signaling Technology, #9455; 1:1000), p-S6K (rabbit monoclonal; Cell Signaling Technology, #9234; 1:1000), p-S6 (rabbit monoclonal; Cell Signaling Technology, #4857; 1:1000), p-H2AX (rabbit monoclonal; Cell Signaling Technology, #9718; 1:200,000), Ki67 (rabbit monoclonal; Thermo Scientific, #RM-9106-FO; 1:500), germ cell nuclear antigen (GCNA; 1:200 IHC) (courtesy of George Enders, University of Kansas). Cell counts were performed to quantify the four principal cellular stages of sperm development (spermatogonia, spermatocytes, round spermatids and elongated spermatids). Counts for undifferentiated spermatogonia and round spermatids were facilitated by immunostaining these cell types with Foxo1 and Crem1, respectively, as described in the text. Spermatocytes and elongated spermatids were identified and counted based on their distinct morphology in routinely stained histologic sections. For each cell type, a minimum of twenty tubules (staged from IV to VII) were counted per mouse.

Statistics

Data were graphed and analyzed using GraphPad Prism 5. Two-tailed Student's *t* tests were used to evaluate significance and calculate *P* values, with threshold values as described in the results or figure legends. Error bars represent standard error of mean values. A *P* value of less than 0.05 was considered significant.

Results

Expression of *Rheb* and *RhebL1* in the gonad and the adult germline

We first characterized the expression of *Rheb* and its closest homolog in the murine genome, *RhebL1* (52% identical and 73% similar at the amino acid level). We took advantage of a previously described microarry-based platform for digital Northern analysis of reproductive tissues and cell types (Gallardo *et al.* 2007b, Contreras *et al.* 2010). The samples subjected to expression profiling included wild-type and *Foxo3* null ovaries at postnatal day (PD) 1, 4, 7, 14 (selected because primordial follicles make up a disproportionately greater fraction of the ovarian mass early in life, leading to good representation of primordial follicle transcripts). In addition, laser-capture microdissected (LCM) oocytes and surrounding granulosa cells from primary to secondary follicles (i.e. early growing follicles) were included given the important role of the mTOR/PI3K pathway in early follicle growth (John *et al.* 2008, Adhikari *et al.* 2009, Adhikari *et al.* 2010). Other samples included superovulated eggs, ES cells, normal testis, germ-cell deficient Sl/Sl(d) testes, E11 embryos, and diverse adult tissues (Fig. 1).

Vasa (a.k.a.) *Ddx4* was included as a representative germ cell-specific control validating the samples and methodology. *Vasa* was expressed in all PD1-14 ovarian samples and in LCM oocytes, but was expressed at low (nearly baseline) levels in the adult ovary, consistent with the fact that oocytes make up only a very small percentage of the ovarian mass (Gallardo *et al.* 2007b). Among adult tissues *Vasa*, was expressed at high levels only in the testis (only tall peak in the right half of the panel) but nearly absent in germ cell-deficient testes, as expected given *Vasa's* germ cell-specific expression. In contrast, *Rheb* was much more broadly expressed with high expression across all tissues, including ovaries and testis where it appears to be expressed in both the germline and somatic cells. In contrast, *RhebL1* was expressed at lower overall apparent levels overall (with lower signal strengths) but like *Rheb* also very broadly expressed. Whereas *Rheb* was represented on the array by a single probe, *RhebL1* was represented by two separate probes. Note that the expression peaks from the second probe are virtually superimposable on the first, consistent with faithful readout of gene expression levels across probes. Neither *Rheb* nor *RhebL1* were differentially expressed in *Foxo3* null ovaries (red bars), arguing that neither gene is a direct *Foxo3* target. Thus in summary, *Rheb* is expressed in gonads and the female germline, making it a plausible candidate for a biological role in the germline.

Conditional inactivation of *Rheb* in the germline with *Vasa-Cre*

A floxed *Rheb* allele ($Rheb^{f}$) was crossed with the germ cell specific Cre recombinase, *Vasa-Cre*. This strategy allows for prenatal deletion of *Rheb* in both the male and female germlines, as *Vasa-Cre* is expressed in both male and female germ cells beginning at

embryonic day 15 (E15) (Gallardo *et al.* 2007a). Available PCR genotyping protocols permit specific amplification of the wild-type, floxed, and null (i.e. Cre-recombined) Rheb alleles. Confirmation of *Vasa-Cre* mediated excision of the floxed third exon of the *Rheb* locus was performed through PCR genotyping of both the *Rheb* floxed and *Rheb*-null alleles in *Vasa-Cre; Rheb*$^{f/+}$ mice. Both the wild type and floxed *Rheb* alleles were detected in multiple tissues of *Vasa-Cre; Rheb*$^{f/+}$ mice, however, the floxed allele was clearly less abundant in the testis, consistent with germ cell Cre recombination and *Rheb* inactivation (Fig. 2 A). The *Rheb* null allele was detected in the testis of the *Vasa-Cre; Rheb*$^{f/+}$ mouse but not in other tissues (Fig. 2 B) again consistent with germ cell specific Cre activity. Germline transmission of the *Rheb* null allele was also confirmed by genotyping progeny from *Vasa-Cre; Rheb*$^{f/-}$ females crossed to wild type males; all progeny carried the null allele (n=18), confirming efficient, biallelic ablation of *Rheb* within oocytes.

Gross and histological analyses of gonads from male and female *Rheb* conditional knockout (cKO) mice

By gross examination, adult *Rheb* cKO (*Vasa-Cre; Rheb*$^{f/-}$) testes were much smaller than those of *Vasa-Cre* negative (*Rheb*$^{f/-}$) sibling controls (Fig. 3 A). A progressive atrophy of the testes was observed in experimental males. *Vasa-Cre; Rheb*$^{f/-}$ testis weights underwent a further two-fold decrease in weight from three to five months of age (Fig. 3 B). Testis sections from three month old *Vasa-Cre; Rheb*$^{f/-}$ males exhibited hypospermatogenesis with all stages of sperm present. However, in aged mice the seminiferous tubules were more severely affected by the loss of *Rheb*. At five months of age, there was severely decreased spermatogenesis and while spermatocytes were present, very few round or elongated spermatids were observed (Fig. 3 C). In contrast, *Vasa-Cre; Rheb*$^{f/-}$ ovaries were grossly unremarkable (Fig. 4 A). Histological analysis of ovary sections showed the presence of growing follicles of all stages (Fig. 4 B) and a healthy pool of quiescent primordial follicles (Fig. 4 C).

Rheb cKO males have decreased sperm counts and abnormal sperm morphology

A complete sperm workup was performed to identify defects in total sperm count, morphology and motility. Epididymides from both *Vasa-Cre; Rheb*$^{f/-}$ and *Rheb*$^{f/-}$ controls were examined histologicaly for the presence of mature spermatozoa (Fig. 5 A). Quantification of sperm head density clearly showed a progressive age-dependent decrease of sperm production (Fig. 5 B). This decrease was also quantified through epididymal sperm concentration counts (Fig. 5 C). By four months of age the *Vasa-Cre; Rheb*$^{f/-}$ males exhibited severe oligoasthenoteratozoospermia. The predominant morphological defect observed was amorphous head shapes (Fig. 5 D).

Rheb is required for male, but not female, fertility

To quantify the effect of *Rheb* cKO on fertility, breeding assays were set up for *Vasa-Cre; Rheb*$^{f/-}$ males and females and *Rheb*$^{f/-}$ sibling controls. The *Rheb* cKO female mice were fertile; their fecundity was indistinguishable from controls and they continued to have litters of normal size up to eighteen weeks of age (Fig. 6 A, B). The male *Rheb* cKO mice, however, did not produce any offspring over a period of twenty weeks (Fig. 6 C, D). This

complete male infertility is expected given the oligoasthenoteratozoospermia observed above.

Histomorphometric analyses of gametogenesis expose a defect in meiotic progression

As an initial characterization of the disrupted seminiferous tubules, and to identify potential developmental blocks in spermatogenesis, cell counts were performed to quantify numbers of spermatogonia, spermatocytes, round spermatids and elongated spermatids (Fig. 7 A). Foxo1 expression was used as a convenient marker of undifferentiated spermatogonia (Goertz *et al.* 2011, Tarnawa *et al.* 2013). Immunostaining and counts revealed normal numbers of undifferentiated spermatogonia in *Vasa-Cre; Rheb*$^{f/-}$ testes at all time points (Fig. 7 C). Spermatocytes were counted based on their large size and distinctive cellular morphology. A significant accumulation of spermatocytes was observed at two months but numbers reverted to normal at three and four month time points. By five months of age, a significant decrease in spermatocyte numbers was observed (Fig. 7 D). Quantifications of round and elongated spermatids were performed through Crem1 immunostaining and cellular morphology, respectively (Delmas *et al.* 1993) (Fig. 7 B). Decreases in round and elongated spermatid counts were observed at early time points (Fig. 7 C, D). Thus in summary, *Rheb* cKO males exhibited a striking age-dependent decrease in spermatid production and a more modest decrease in spermatocytes, while maintaining normal numbers of undifferentiated spermatogonia. These results point to abnormalities in meiotic progression.

Spermatogonia continue to proliferate and initiate meiosis

In light of the progressive decrease in spermatocytes in the *Vasa-Cre; Rheb*$^{f/-}$ mice, proliferation and meiotic entry were further evaluated by immunostaining for Ki67 and pH2AX, respectively. Ki67 is a marker of actively cycling cells, while H2AX is phosphorylated in response to double-stranded DNA breaks (Hamer *et al.* 2002, Akbay *et al.* 2013). Phosphorylated H2AX (pH2AX) nuclear foci serve as a marker of meiotic recombination in response to the formation of chiasma between sister chromatids in leptotene spermatocytes. However, detailed counts of cells positive for Ki67 and pH2AX foci revealed no significant differences between *Vasa-Cre; Rheb*$^{f/-}$ and control males at all time points studied (Fig. 8). Therefore, spermatogonial proliferation and meiotic entry *per se* appears largely unaffected in *Rheb* cKO males, again consistent with a severe defect in meitoic progression.

The activation status of mTOR, S6K and 4EBP appears to be unaffected in *Vasa-Cre; Rheb*$^{f/-}$ mice

We then sought to determine the activation status of mTOR pathway components in *Rheb* cKO testes as well as ovaries. Immunohistochemistry was performed for phosphorylated (i.e. activated) mTOR pathway members p-mTOR, p-S6K, p-S6 and p-4EBP using well-validated phosphorylation site-specific antibodies for each of these factors. However, no significant differences were observed in the phosphorylation state of any of these mTOR pathway components in *Rheb* cKO vs. control testes, as gauged by staining intensity, when specific spermatogenic stages were compared (Fig. 9).

Discussion

These studies document a male infertility phenotype associated with multiple defects in the meiotic and post-meiotic stages of spermatogenesis in mice with conditional genetic inactivation of *Rheb* in the germ line. Interestingly, given prior studies implicating mTORC1 in stem cell self-renewal, Rheb was dispensable for spermatogonial self-renewal and mitotic proliferation (Hobbs *et al.* 2010). However, *Rheb* was necessary for spermiogenesis, as *Rheb* males exhibited greatly reduced epididymal sperm numbers, and the few sperm present were immotile and exhibited grossly abnormal head morphology. A delay in meiotic progression was also evident at two months of age as spermatocyte counts were significantly increased. Immunostains for meiotic initiation-associated double-strand DNA breaks were relatively unaffected, further suggesting that these defects were due to delays or abnormalities in meiotic progression, and not meiotic initiation per se. Interestingly, these pleiotropic phenotypes were age-dependent, and in five month-old males, the meiotic defect was even more severe, with greatly decreased numbers of post-meiotic spermatids.

A large number of mouse mutants with combined defects in meiosis and spermiogenesis have been described. These mutations affect a wide range of processes, from acrosome and tail formation to misregulation of late spermiogenesis gene expression (Yan 2009). The multiple defects that we have described resemble in several respects the spermatogenesis phenotype previously described for mice with conditional germ line inactivation of *Dicer*, the miRNA processing enzyme (Korhonen *et al.* 2011, Romero *et al.* 2011). The *Dicer* cKO is also infertile due to cumulative defects in meiosis and spermiogenesis that result in an oligoasthenoteratozoospermia phenotype. Delayed progression of meiosis was also observed but the phenotype was manifest during the first wave of spermatogenesis and did not worsen with age (Romero *et al.* 2011). Both Rheb and Dicer control critical pathways regulating protein expression, albeit through two fundamentally different mechanisms. The biological basis of these *Rheb* and *Dicer* male infertility phenotypes likely resides in this precise regulation of gene expression and translation required to complete the complex transcription-independent processes of meiotic and post-meiotic sperm development. With hundreds of testis-specific genes expressed in spermatocytes and spermatids, the translation of these mRNAs must be perfectly orchestrated to coordinate acrosome biogenesis, tail formation, nuclear condensation and cytoplasm removal. With the loss of functional spermatozoa in *Vasa-Cre; Rheb*$^{f/-}$ function in the testis, it is reasonable to hypothesize that regulation of protein translation by mTORC1 is required for spermiogenesis. Although we did not document an obvious defect in spermatogonial function, and the numbers of these cells were unaffected, it is possible that Rheb inactivation resulted in some unidentified abnormality (metabolic, transcriptional, etc.) in early stages of spermatogenesis that became manifest at later steps of spermatogenesis.

With regards to the control of protein translation, Rheb and mTORC1 act through canonical pathways including the phosphorylation of 4EBP and S6K. We were unable to document, by in situ methods or Western blotting, significant alterations in the phosphorylation state of these key mTOR effectors. Several possibilities may be considered. First, by Western blotting, the significant somatic cell contamination of whole testes lysates could make it difficult to detect differences in phosphorylation levels (we observed no differences through

these methods - unpublished data). We also failed to detect differences in the phosphorylation levels in these factors (and hence significant alterations in mTORC1 signaling) by potentially more sensitive in situ methods, although immunohistochemistry may also be insensitive to relatively modest changes in target epitope levels. It is also possible that unknown feedback loops serve to preserve Tsc/mTOR signaling in the absence of Rheb. Although a precise molecular mechanism of action was not determined, the *Rheb* cKO is the first genetic *in vivo* study which implicates Rheb in the regulation of spermatogenesis.

Despite the complete sterility of *Rheb* cKO males, cKO females were fertile and exhibited normal fecundity. We observed no alterations in primordial follicle numbers, or follicle maturation, by careful histologic analyses. This result is somewhat surprising in light of previous studies clearly demonstrating a central role of mTOR signaling in the regulation of primordial follicle activation. The global follicle activation phenotype previously documented in *Tsc1* or *Tsc2* cKO females was associated with dramatic upregulation of the mTOR signaling pathway (demonstrable with the same immunohistochemical assays performed in our study) (Adhikari *et al.* 2009, Adhikari *et al.* 2010), yet *Rheb* conditional inactivation in oocytes did not have any observable effect on follicle maturation. Although different Cre deletor lines were used in these studies (*Vasa-Cre* and *Gdf9-Cre*), this does not appear to provide an adequate explanation, as both Cre deletor lines have been extensively utilized and well-documented to lead to efficient Cre-mediated recombination in primordial oocytes (Castrillon *et al.* 2003, Lan *et al.* 2004, Gallardo *et al.* 2007a, Adhikari *et al.* 2009). If mTORC1 activation played an essential role in the recruitment of primordial follicles, then Rheb inactivation would be predicted to result in a primordial follicle arrest phenotype in the absence of mTOR signaling secondary to Rheb inactivation. Explanations for the lack of phenotype may include the action, within the oocyte, of functionally-redundant members of the GTPase superfamily, such as the Rheb homolog RhebL1. Although global *RhebL1* knockout mice were viable and fertile (Zou *et al.* 2011), we have documented RhebL1 expression in the oocyte (Fig. 1 C, D), which could serve to compensate for the failure of complete Rheb inactivation to affect any necessary thresholds of mTOR activation (Tee *et al.* 2005). A *Rheb* germ cell cKO in a *RhebL1* null background may provide insights into this hypothesis. Alternately, an unknown Rheb homolog, or perhaps a more distantly-related Ras-like GTPase may provide this function. Furthermore, cellular functions including the control of apoptosis, differentiation, and the actin cytoskeleton regulation have been proposed to be modulated by non-canonical (i.e. mTORC1-independent) functions of Tsc1/Tsc2 (Neuman & Henske 2011) and it is possible that such mTOR-independent actions of the Tsc complex also contribute to the lack of a *Rheb* ovarian phenotype.

Acknowledgments

Funding

The project described was supported by Award Number R01HD048690 from the Eunice Kennedy Shriver National Institute of Child Health & Human Development. The content is solely the responsibility of the authors and does not necessarily represent the official views of the Eunice Kennedy Shriver National Institute of Child Health & Human Development or the National Institutes of Health.

We thank Paul F. Worley (Johns Hopkins University School of Medicine) and Bo Xiao (Sichuan University) for the *Rheb* floxed mice. We thank Delali Bassowou for technical assistance, as well as Kent Hamra and Rolf Brekken for helpful discussions.

References

Adhikari D, Flohr G, Gorre N, Shen Y, Yang H, Lundin E, Lan Z, Gambello MJ, Liu K. Disruption of Tsc2 in oocytes leads to overactivation of the entire pool of primordial follicles. Mol Hum Reprod. 2009; 15:765–770. [PubMed: 19843635]

Adhikari D, Zheng W, Shen Y, Gorre N, Hamalainen T, Cooney AJ, Huhtaniemi I, Lan ZJ, Liu K. Tsc/mTORC1 signaling in oocytes governs the quiescence and activation of primordial follicles. Hum Mol Genet. 2010; 19:397–410. [PubMed: 19843540]

Akbay EA, Pena CG, Ruder D, Michel JA, Nakada Y, Pathak S, Multani AS, Chang S, Castrillon DH. Cooperation between p53 and the telomere-protecting shelterin component Pot1a in endometrial carcinogenesis. Oncogene. 2013; 32:2211–2219. [PubMed: 22689059]

Castrillon DH, Miao L, Kollipara R, Horner JW, DePinho RA. Suppression of ovarian follicle activation in mice by the transcription factor Foxo3a. Science. 2003; 301:215–218. [PubMed: 12855809]

Contreras CM, Akbay EA, Gallardo TD, Haynie JM, Sharma S, Tagao O, Bardeesy N, Takahashi M, Settleman J, Wong KK, Castrillon DH. Lkb1 inactivation is sufficient to drive endometrial cancers that are aggressive yet highly responsive to mTOR inhibitor monotherapy. Dis Model Mech. 2010; 3:181–193. [PubMed: 20142330]

Delmas V, van der Hoorn F, Mellstrom B, Jegou B, Sassone-Corsi P. Induction of CREM activator proteins in spermatids: down-stream targets and implications for haploid germ cell differentiation. Mol Endocrinol. 1993; 7:1502–1514. [PubMed: 8114765]

Fingar DC, Blenis J. Target of rapamycin (TOR): an integrator of nutrient and growth factor signals and coordinator of cell growth and cell cycle progression. Oncogene. 2004; 23:3151–3171. [PubMed: 15094765]

Gallardo T, Shirley L, John GB, Castrillon DH. Generation of a germ cell-specific mouse transgenic Cre line, Vasa-Cre. Genesis. 2007a; 45:413–417. [PubMed: 17551945]

Gallardo TD, John GB, Bradshaw K, Welt C, Reijo-Pera R, Vogt PH, Touraine P, Bione S, Toniolo D, Nelson LM, Zinn AR, Castrillon DH. Sequence variation at the human FOXO3 locus: a study of premature ovarian failure and primary amenorrhea. Hum Reprod. 2008; 23:216–221. [PubMed: 17959613]

Gallardo TD, John GB, Shirley L, Contreras CM, Akbay EA, Haynie JM, Ward SE, Shidler MJ, Castrillon DH. Genomewide discovery and classification of candidate ovarian fertility genes in the mouse. Genetics. 2007b; 177:179–194. [PubMed: 17660561]

Goertz MJ, Wu Z, Gallardo TD, Hamra FK, Castrillon DH. Foxo1 is required in mouse spermatogonial stem cells for their maintenance and the initiation of spermatogenesis. J Clin Invest. 2011; 121:3456–3466. [PubMed: 21865646]

Hamer G, Roepers-Gajadien H, Duyn-Goedhart A, Gademan I, Kal H, Buul P, Rooij D. DNA Double-Strand Breaks and -H2AX Signaling in the Testis. Biol Reprod. 2002; 68:628–634. [PubMed: 12533428]

Hobbs RM, Seandel M, Falciatori I, Rafii S, Pandolfi PP. Plzf regulates germline progenitor self-renewal by opposing mTORC1. Cell. 2010; 142:468–479. [PubMed: 20691905]

Hosaka T, Biggs WH 3rd, Tieu D, Boyer AD, Varki NM, Cavenee WK, Arden KC. Disruption of forkhead transcription factor (FOXO) family members in mice reveals their functional diversification. Proc Natl Acad Sci U S A. 2004; 101:2975–2980. [PubMed: 14978268]

John GB, Gallardo TD, Shirley LJ, Castrillon DH. Foxo3 is a PI3K-dependent molecular switch controlling the initiation of oocyte growth. Dev Biol. 2008; 321:197–204. [PubMed: 18601916]

John GB, Shirley LJ, Gallardo TD, Castrillon DH. Specificity of the requirement for Foxo3 in primordial follicle activation. Reproduction. 2007; 133:855–863. [PubMed: 17616716]

Korhonen HM, Meikar O, Yadav RP, Papaioannou MD, Romero Y, Da Ros M, Herrera PL, Toppari J, Nef S, Kotaja N. Dicer is required for haploid male germ cell differentiation in mice. PLoS One. 2011; 6:e24821. [PubMed: 21949761]

Lan ZJ, Xu X, Cooney AJ. Differential oocyte-specific expression of Cre recombinase activity in GDF-9-iCre, Zp3cre, and Msx2Cre transgenic mice. Biol Reprod. 2004; 71:1469–1474. [PubMed: 15215191]

Laplante M, Sabatini DM. mTOR signaling at a glance. J Cell Sci. 2009; 122:3589–3594. [PubMed: 19812304]

Neuman NA, Henske EP. Non-canonical functions of the tuberous sclerosis complex-Rheb signalling axis. EMBO Mol Med. 2011; 3:189–200. [PubMed: 21412983]

Reddy P, Liu L, Adhikari D, Jagarlamudi K, Rajareddy S, Shen Y, Du C, Tang W, Hamalainen T, Peng SL, Lan ZJ, Cooney AJ, Huhtaniemi I, Liu K. Oocyte-specific deletion of Pten causes premature activation of the primordial follicle pool. Science. 2008; 319:611–613. [PubMed: 18239123]

Romero Y, Meikar O, Papaioannou MD, Conne B, Grey C, Weier M, Pralong F, De Massy B, Kaessmann H, Vassalli JD, Kotaja N, Nef S. Dicer1 depletion in male germ cells leads to infertility due to cumulative meiotic and spermiogenic defects. PLoS One. 2011; 6:e25241. [PubMed: 21998645]

Schneider CA, Rasband WS, Eliceiri KW. NIH Image to ImageJ: 25 years of image analysis. Nat Methods. 2012; 9:671–675. [PubMed: 22930834]

Sullivan SD, Castrillon DH. Insights into primary ovarian insufficiency through genetically engineered mouse models. Semin Reprod Med. 2011; 29:283–298. [PubMed: 21972066]

Tarnawa ED, Baker MD, Aloisio GM, Carr BR, Castrillon DH. Gonadal expression of foxo1, but not foxo3, is conserved in diverse Mammalian species. Biol Reprod. 2013; 88:103. [PubMed: 23486915]

Tee AR, Blenis J, Proud CG. Analysis of mTOR signaling by the small G-proteins, Rheb and RhebL1. FEBS Lett. 2005; 579:4763–4768. [PubMed: 16098514]

Tzivion G, Dobson M, Ramakrishnan G. FoxO transcription factors; Regulation by AKT and 14-3-3 proteins. Biochim Biophys Acta. 2011; 1813:1938–1945. [PubMed: 21708191]

Wyrobek AJ, Bruce WR. Chemical induction of sperm abnormalities in mice. Proc Natl Acad Sci U S A. 1975; 72:4425–4429. [PubMed: 1060122]

Yan W. Male infertility caused by spermiogenic defects: lessons from gene knockouts. Mol Cell Endocrinol. 2009; 306:24–32. [PubMed: 19481682]

Zou J, Zhou L, Du XX, Ji Y, Xu J, Tian J, Jiang W, Zou Y, Yu S, Gan L, Luo M, Yang Q, Cui Y, Yang W, Xia X, Chen M, Zhao X, Shen Y, Chen PY, Worley PF, Xiao B. Rheb1 is required for mTORC1 and myelination in postnatal brain development. Dev Cell. 2011; 20:97–108. [PubMed: 21238928]

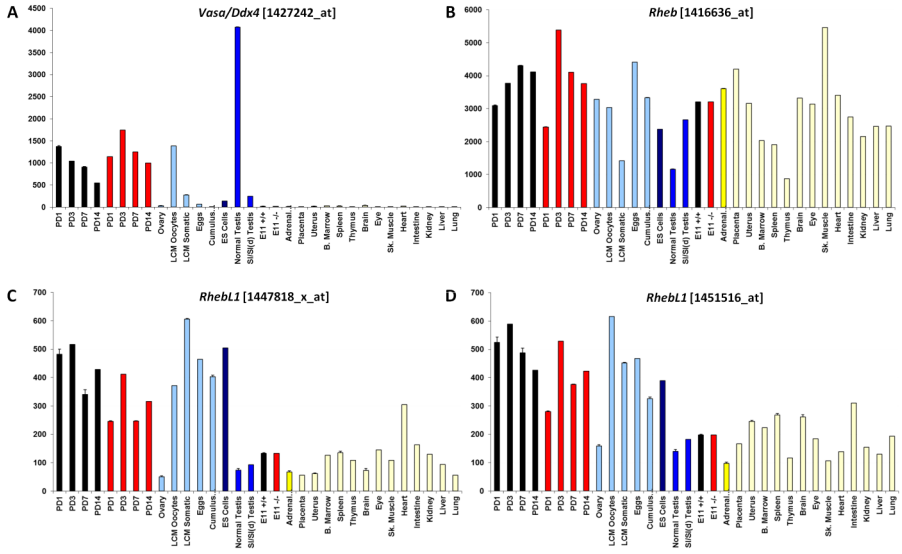

Figure 1. RNA expression analysis of *Rheb* and *RhebL1*

Graphs show relative expression levels of single probe set for indicated gene across multiple samples; error bars represent SEM. Samples are (left to right) *Foxo3* +/+ PD1, -3, -7, -14 (black), *Foxo3* −/− PD1, -3, -7, -14 (red), adult ovary, laser-capture microdissected (LCM) primary and secondary oocytes, LCM somatic cells (primary plus secondary granulosa cells and surrounding stroma), eggs, cumulus cells, ES cells, normal adult testis, Sl/Sld (germ cell-depleted) adult testis, *Foxo3* +/+ E11 embryos, *Foxo3* −/− E11 embryos, adrenal gland, placenta, uterus, bone marrow, spleen, thymus, brain, eye, skeletal muscle, heart, intestine, kidney, liver, and lung. (A) Vasa/Ddx4 as representative control (germ cell-specific gene in both males and females). (B) *Rheb*. (C) *RhebL1* (probe set #1). (D) *RhebL1* (probe set #2).

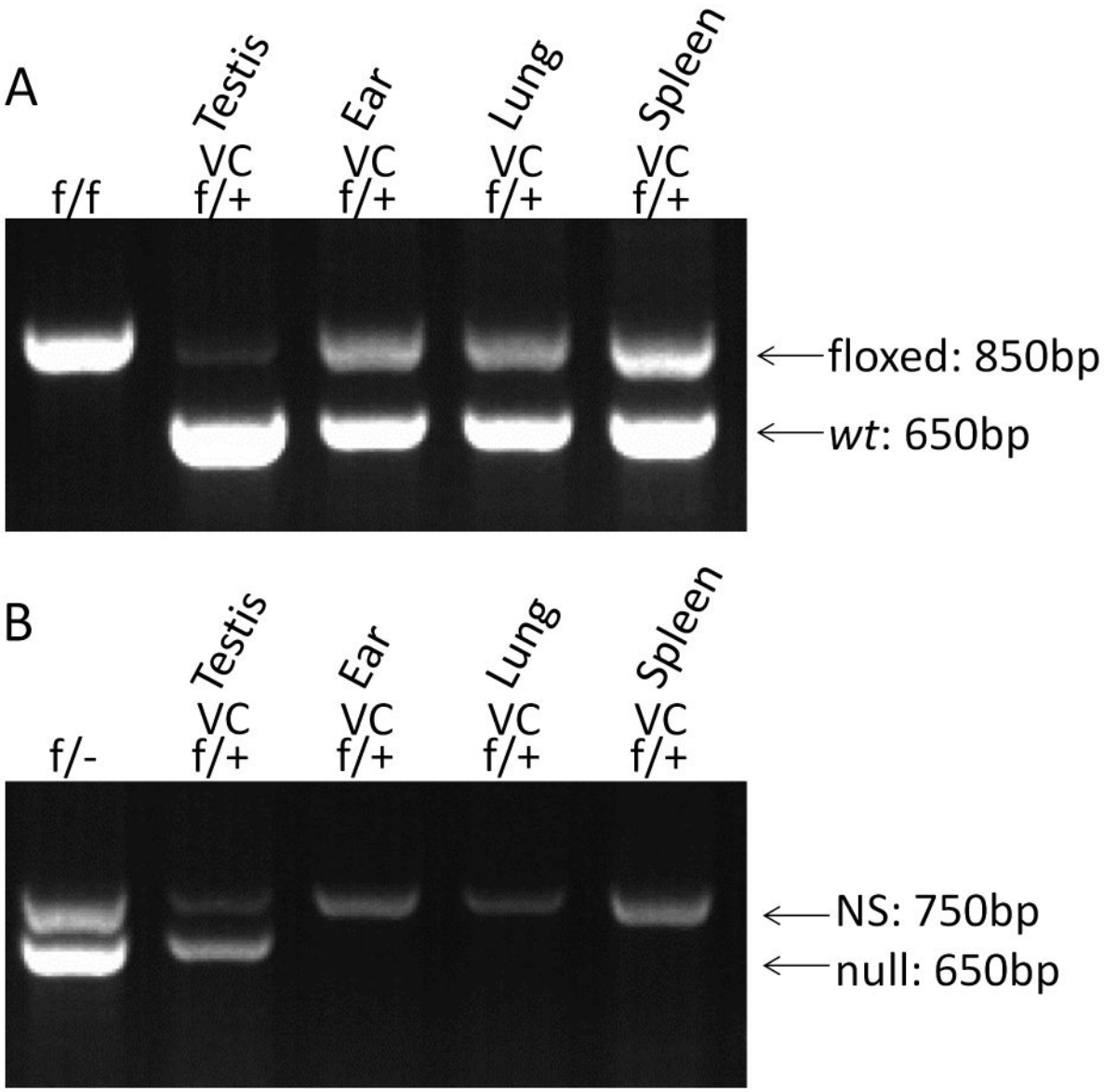

Figure 2. Genotype confirmation of germ cell *Rheb* conditional knockout

(A) An ethidium bromide-stained 1% agarose gel shows the presence of the *Rheb*-floxed allele (850 bp) in tail DNA from a *Rheb* homozygous floxed mouse as well as all other tissues of a *Vasa-Cre; Rheb*$^{f/+}$ (heterozygous) male. The floxed (f) band is decreased in the *Vasa-Cre; Rheb*$^{f/+}$ testis consistent with *Vasa-Cre* mediated recombination in germ cells. The *wt* (+) band (650bp) is observed in tissues from this heterozygous male mouse, as expected. (B) Cre-mediated excision was further confirmed by the presence of the *Rheb* null allele (650bp) in a *Vasa-Cre; Rheb*$^{f/+}$ testis as well as a *Rheb*$^{f/-}$ control testis. The *Rheb* null allele was not detected in other tissues (e.g. skin, lung, and spleen). NS=non-specific PCR product (~750bp).

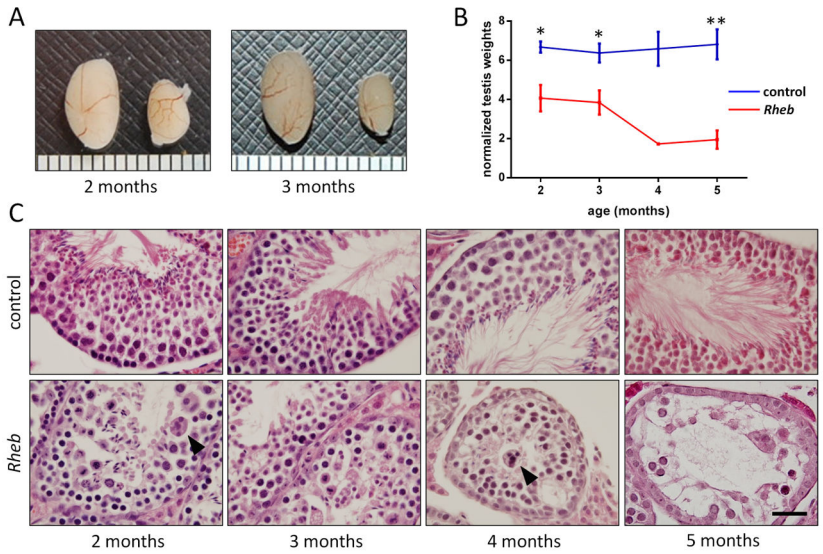

Figure 3. Conditional *Rheb* inactivation results in a progressive defect of spermatogenesis

(A) Intact testes. Right=*Vasa-Cre; Rheb*$^{f/-}$; Left=*Rheb*$^{f/-}$ sibling control. Ruler markings = 1 mm. (B) Testis weights in mice of different ages. Red=*Vasa-Cre; Rheb*$^{f/-}$; Blue=*Rheb*$^{f/-}$ sibling control. *$P < 0.05$, **$P < 0.005$, by unpaired T test (two months, n = 2; three months, n = 3; four months, n = 1 [no statistical test performed]; five months, n = 3) (C) H&E stained tissue sections from testes of two to five month-old *Rheb* cKO and sibling control mice. Representative fields illustrate an abnormal organization of seminiferous tubules at the two month time point and the age dependent defect in meiotic progression resulting in the progressive loss of round and elongating spermatids in the 5 month old testis. Arrowheads indicate large multinucleated germ cells. Bar=50 μm.

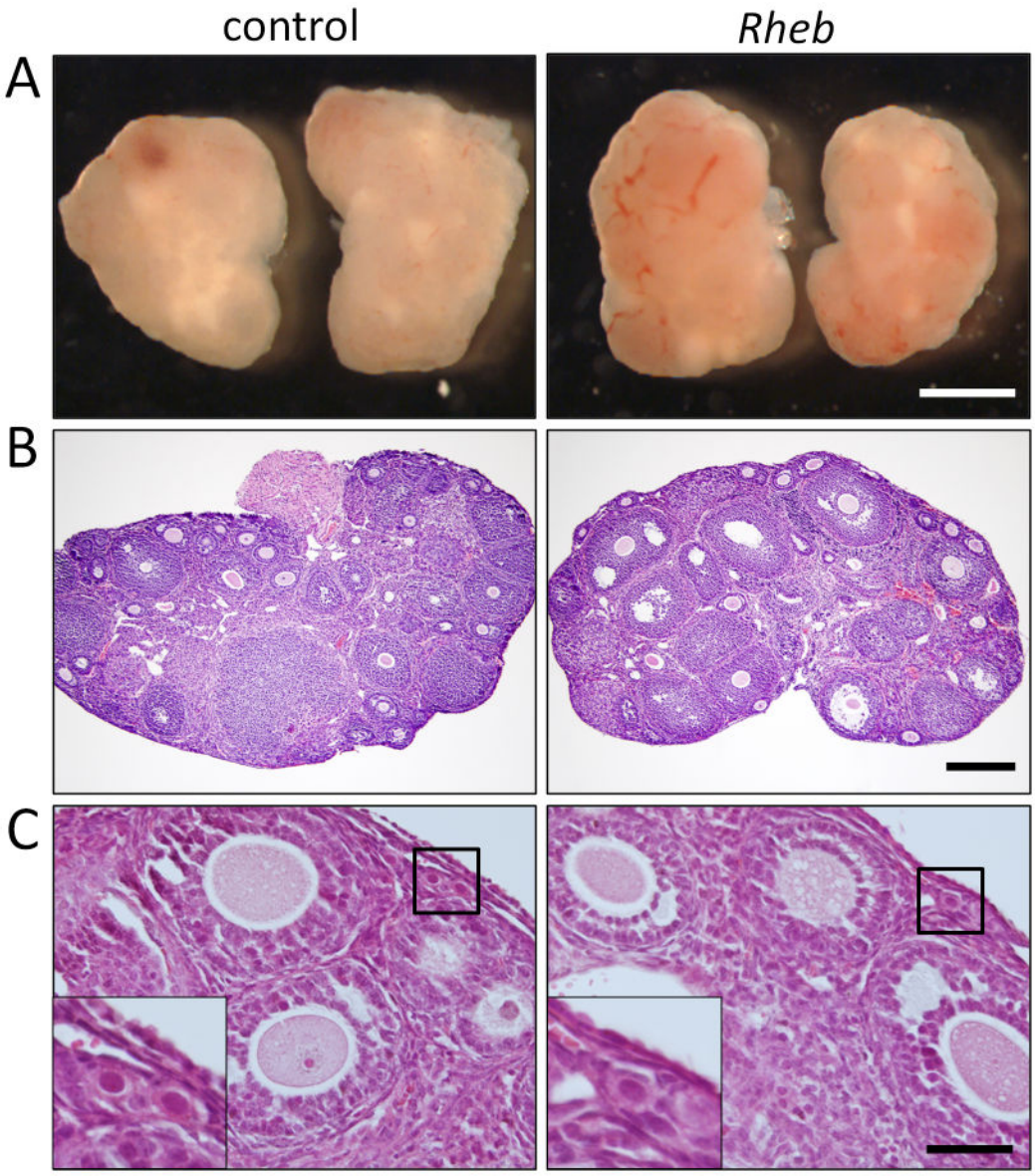

Figure 4. Ovaries of *Rheb* cKO mice are grossly normal and contain growing follicles of all stages as well as morphologically-normal primordial follicles

(A) Intact ovaries of *Rheb* cKO (*Vasa-Cre; Rheb*$^{f/-}$) females were of similar size and shape relative to sibling (*Rheb*$^{f/-}$) controls. Bar = 1 mm. (B) H&E stained tissue sections from *Rheb* cKO and sibling control ovaries revealed growing follicles of all stages. Bar = 250 μm. (C) Higher magnification shows growing primary and secondary follicles. Insets: morphologically normal, quiescent, primordial follicles. Scale bar = 50 μm.

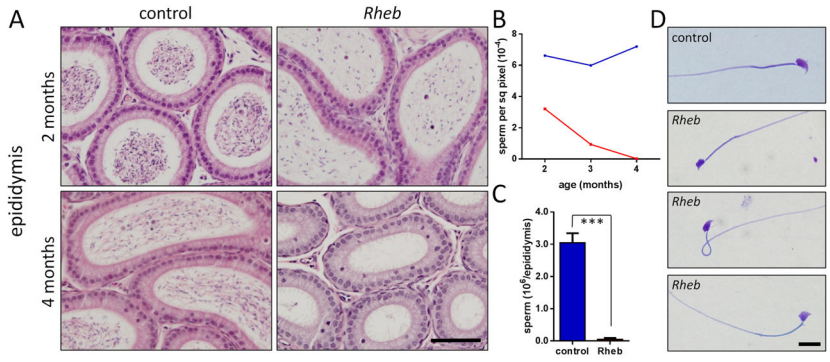

Figure 5. Total sperm production is drastically decreased and remaining sperm are malformed

(A) Histology of epididymides from control and experimental mice. Bar = 100 μm. (B) The decrease in epididymal sperm was quantified by sperm head density counts (n = 1 for all time points and genotypes). (C) Total sperm counts were performed after releasing the sperm from the epididymis. ***$P < 0.0001$. Red=*Vasa-Cre; Rheb*$^{f/-}$ n = 4; Blue=*Rheb*$^{f/-}$ n = 5 sibling controls. (D) The few sperm obtained from the epididymis of *Rheb* cKO mice were all immotile and exhibited abnormal morphology. Bar = 10 μm; all panels at same magnification.

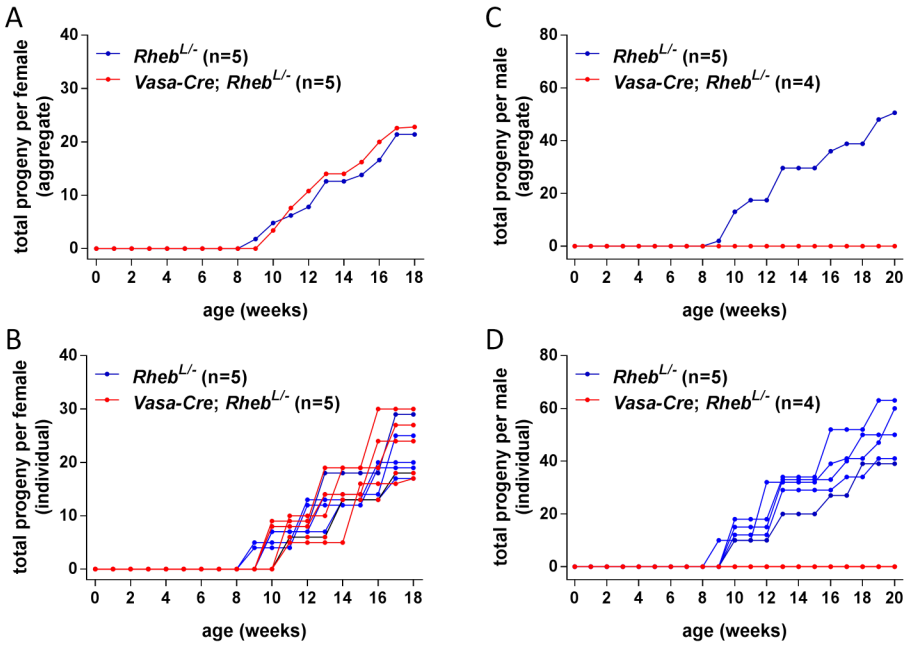

Figure 6. Serial breeding assays reveal that *Rheb* cKO males are sterile while *Rheb* cKO females are fertile with normal fecundity to 18 weeks of age

(A) Aggregate (i.e. all animals of the same genotype averaged) and (B) Individual (i.e. every line represents a single animal) representations of total progeny per female. (B) Aggregate and (C) Individual representations of total progeny per male.

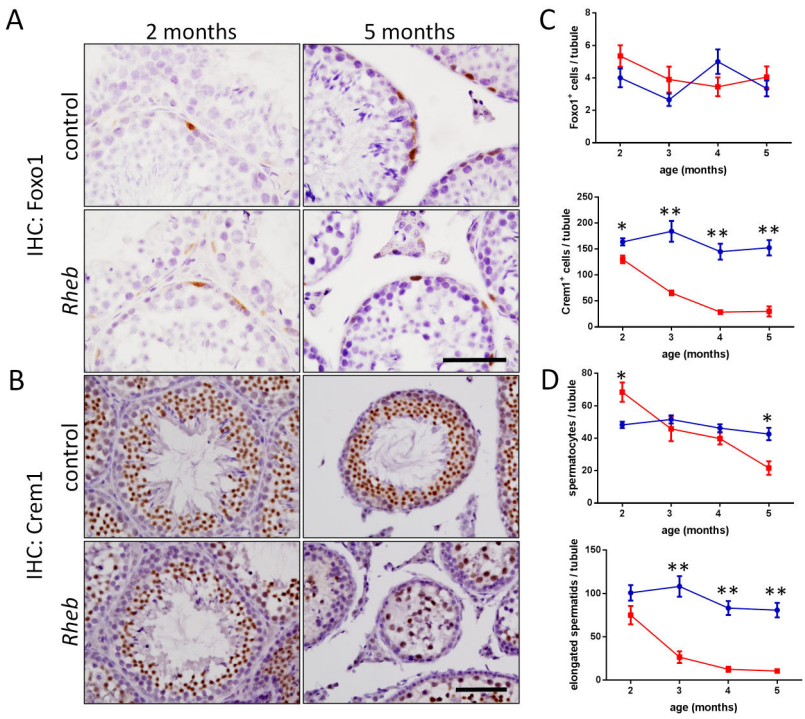

Figure 7. Cell counts reveal meiotic progression defect

(A) Foxo1 and (B) Crem1 immunostains of *Rheb* cKO (*Vasa-Cre; Rheb*$^{f/-}$) and control testes at two and five months of age. Bar = 50 μm and 100 μm, respectively. (C) Quantification of Foxo1 and Crem1 positive cell counts in twenty tubules; *$P < 0.05$, **$P < 0.0005$ by unpaired T test. (D) Counts of spermatocytes and spermatids in hematoxylin-stained tissue sections. The counts of elongated spermatids closely mirrored the observed decrease in Crem1^{+} round spermatids; *$P < 0.05$, **$P < 0.005$, ***$P < 0.0005$, by unpaired T test.

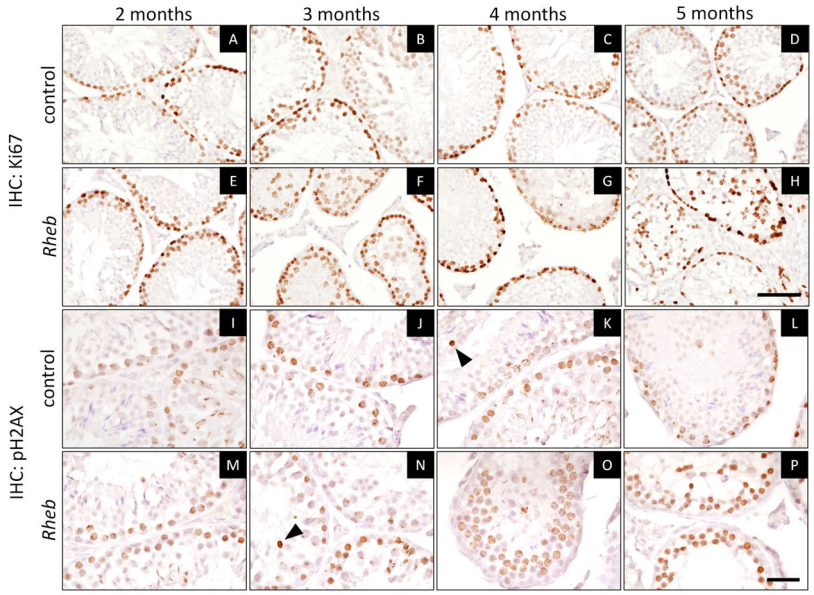

Figure 8. Analyses of cell proliferation and meiotic entry

(A–H) Immunostaining for Ki67 as a marker for cellular proliferation. Bar=100 μm (I–P) Immunostaining for pH2AX as a marker of meiotic entry. Scattered apoptotic germ cells server as an internal positive control (arrowheads) since apoptotic cells undergo DNA fragmentation and are strongly positive for pH2AX. Bar = 25 μm.

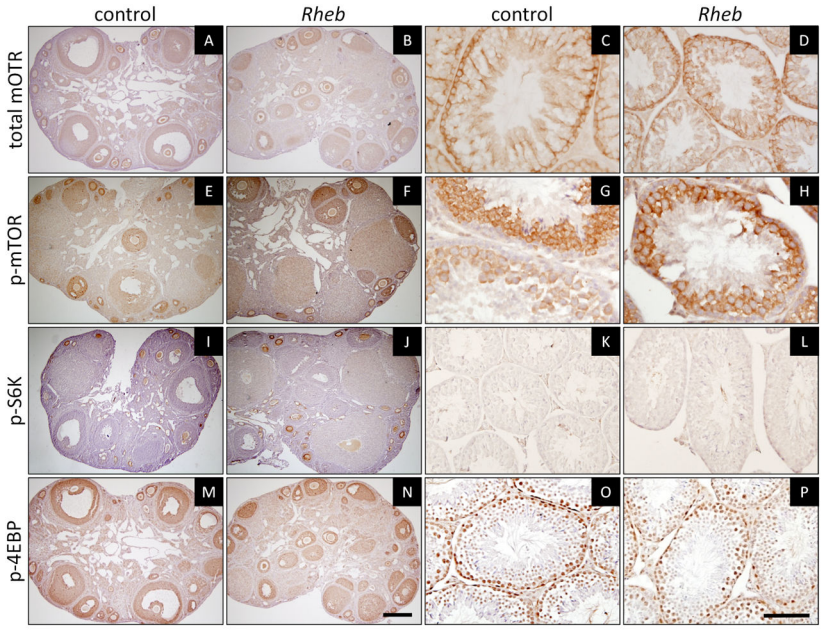

Figure 9. Analysis of mTOR and downstream effectors

Immunostains with phosphorylation-site specific antibodies against canonical mTOR pathway members in both ovaries (left) and testes (right). Bar = 250 μm and 100 μm, respectively. (A–D) Total mTOR. (E–H) p-mTOR. (I–L) p-S6K. (M–P) p-4EBP.